

miR-96 Regulates Liver Tumor-Initiating Cells Expansion and Sorafenib Resistance

Yonggang Huang

kunshan of traditional chinese hospital

Jin Zhang

second military medical university

Wei Dong

second military medical university

Huiping Peng

kunshan of traditional chinese hospital

Maolin Gu

kunshan of traditional chinese hospital

Hengjie Wang (✉ xiaowang198587@163.com)

kunshan of traditional chinese hospital <https://orcid.org/0000-0002-0874-5379>

Primary research

Keywords: hepatocellular carcinoma, tumor-initiating cells, miR-96, SOX6, sorafenib

Posted Date: March 20th, 2020

DOI: <https://doi.org/10.21203/rs.3.rs-18165/v1>

License:  This work is licensed under a Creative Commons Attribution 4.0 International License.

[Read Full License](#)

Abstract

Background Liver tumor-initiating cells (T-ICs) contribute to tumorigenesis, progression, recurrence and drug resistance of hepatocellular carcinoma (HCC). However, the underlying mechanism for the propagation of liver T-ICs remains unclear.

Methods Real-time PCR was used to detect the expression of miR-96 in liver tumor-initiating cells (T-ICs). The impact of miR-96 on liver T-ICs expansion was investigated both in vivo and in vitro . The correlation between miR-96 expression and sorafenib benefits in HCC was further evaluated in patient-derived xenografts (PDXs).

Results Our finding shows that miR-96 is upregulated in liver T-ICs. Functional studies revealed that forced miR-96 promotes liver T-ICs self-renewal and tumorigenesis. Conversely, knockdown miR-96 inhibits liver T-ICs self-renewal and tumorigenesis. Mechanistically, miR-96 downregulates SOX6 via its mRNA 3'UTR in liver T-ICs. Furthermore, the miR-96 expression determines the responses of hepatoma cells to sorafenib treatment. Analysis of patient-derived xenografts (PDXs) further demonstrated that the miR-96 may predict sorafenib benefits in HCC patients.

Conclusion Our findings revealed the crucial role of the miR-96 in liver T-ICs expansion and sorafenib response, rendering miR-96 as an optimal target for the prevention and intervention of HCC.

Background

Hepatocellular carcinoma (HCC) is the most common liver cancer in adults and a challenging disease with poor prognosis (1, 2). The substantial heterogeneity and hierarchical organization in liver cancer support the theory of tumor initiating cells (T-ICs) or cancer stem cells (CSCs) in HCC (3, 4). T-ICs exhibit extended self-renewal potential and tumor initiating ability. Tumors that harbor an abundant T-IC population or have high expression of stemness-related genes may signal a poor clinical outcome in HCC patients (5, 6). Therefore, understanding how liver T-ICs regulate tumor initiation and progression is of key importance for future treatment strategies.

MicroRNAs (miRNAs) are a class of small non-coding RNA molecules, that contain approximately 22 nucleotides (7, 8). miRNAs typically regulate post-transcriptional gene expression by interacting with sequences within the 3'-untranslational region (3'-UTR) of the target mRNA and play important roles in a variety of biological processes, including cell proliferation, differentiation, metastasis and apoptosis (9–11). Numerous studies also found that miRNAs are involved in the initiation, progression and recurrence of various tumors, including lung, liver and bladder cancer. miR-96 has been recognized as an oncogenic miRNA that is upregulated in various types of cancer. Previous studies found that miR-96 promotes metastasis of papillary thyroid cancer through targeting SDHB (12). Moreover, miR-96 also induced non-small-cell lung cancer progression through competing endogenous RNA network and affecting EGFR signaling pathway (13). However, the function of miR-96 in liver T-ICs is unknown.

In the present study, we first found that the expression of miR-96 is upregulated in liver T-ICs. Next, using loss-of-function and gain-of-function analyses in liver T-ICs, we demonstrate that miR-96 can promote the self-renewal capacity and tumorigenicity of liver T-ICs. Further mechanism study reveals that miR-96 directly target SOX6 in liver T-ICs. miR-96 overexpression HCC cells are resistant to sorafenib treatment. The analysis of patient-derived xenografts (PDXs) demonstrated that miR-96 may predict sorafenib benefits in HCC patients. In conclusion, our findings revealed the crucial role of the miR-96 in liver T-ICs expansion and sorafenib response, rendering miR-96 an optimal target for the prevention and intervention in HCC.

Materials And Methods

Patients and samples

The HCC tissues were collected from surgical resections of patients without preoperative treatment at Eastern Hepatobiliary Surgery Hospital (Shanghai, China). A group of 30 HCC specimens were used for analyzing the correlation between miR-96 and SOX6 mRNA expression. Three HCC specimens were used for isolating CD133 and EpCAM positive liver T-ICs. Four specimens were used for patient-derived xenograft (PDX) model. Patient informed consent was obtained and the procedure of human sample collection was approved by the Ethics Committee of Eastern Hepatobiliary Surgery Hospital.

Cell lines and cell culture

Patient-derived primary HCC cultures of tumor cells were obtained from fresh tumor specimens of HCC patients as previously described. The human primary hepatoma cells were isolated by collagenase perfusion and centrifugation. Briefly, the liver cancer tissues were washed several times in pre-cooled sterile PBS buffer containing Red Blood Cell Lysis Buffer and 0.5% collagenase IV to remove blood and connective tissue; GBSS mixed enzyme solution was used for digestion. The cells were centrifuged, and the supernatant was discarded. Cell activity was detected by Trypan Blue staining, and cultured in a bottle containing complete medium heavy suspension at 37°C and 5% CO₂ environment culture. During this process the cell morphology was identified.

The HCC cell line HCCLM3 were purchased from the Chinese Academy of Sciences (Shanghai, China). The HCC cell line CSQT-2 was obtained from professor Shuqun Chen. The HCC cells were cultured with Dulbecco's modified Eagle's medium (DMEM) supplemented with 10% fetal bovine serum (FBS) and 2 mM L-glutamine, and 25 µg/ml of gentamicin and maintained at 37°C in 5% CO₂ incubator. The cultured cells were digested with 0.5% trypsin and moved to a new plate twice a week. miR-96 mimic or miR-96 sponge lentivirus and their control lentivirus were purchased from Shanghai RiboBio (Guangzhou, China). The HCC cells were infected with lentivirus and then screened by puromycin as described before (14). The SOX6 siRNA and its control were obtained from GenePharma (Shanghai, China).

RNA interference

Small interference RNAs (siRNAs) against SOX6 and NC (NC, negative control) siRNA were synthesized by Genepharma (Shanghai, China). The siRNAs were transfected into the hepatoma cells at a final concentration of 200 nM using siRNA transfection reagent according to the manufacturer's instructions (Polyplus, Illkirch, France). The cells were harvested or subjected to further downstream experiments 24-72 hours after transfection. Gene knockdown was validated by western blotting.

Flow-cytometry analysis

For CD133⁺ and EpCAM⁺ cells sorting, primary HCC patients' cells and hepatoma cells were incubated with the primary anti-CD133 (Cat. no. 372806, Biolegend, Inc., San Diego, CA) or anti-EpCAM (Cat. no. ab8666; Abcam, USA) for 30 minutes at room temperature. The cells were then subjected to flow cytometry using a MoFlo XDP cell sorter from Beckman Coulter (Indianapolis, IN, USA) according to the manufacturer's instructions. The sorted cells from three independent experiments were subjected to Real-time PCR assay.

miR-96 mimic or miR-96 sponge and control hepatoma cells were incubated with the primary anti-EpCAM for 30 minutes at room temperature. The flow-cytometry analysis was performed using a MoFlo XDP from Beckman Coulter according to the manufacturer's instructions.

Spheroid formation assay

miR-96 mimic or miR-96 sponge and their control hepatoma cells were cultured in a 96-well ultra-low attachment (300 cells per well) and cultured in DMEM/F12 (Gibco) media, supplemented with 1% FBS, 20 ng/mL bFGF and 20 ng/mL EGF for seven days. The total number of spheres was counted under the microscope (Olympus).

In vitro limiting dilution assay

Various numbers of miR-96 mimic or miR-96 sponge and their control hepatoma cells (2, 4, 8, 16, 32, 64 cells per well, n=16) were seeded into 96-well ultra-low attachment and cultured in DMEM/F12 (Gibco) supplemented with 1% FBS, 20 ng/mL bFGF and 20 ng/mL EGF for seven days. The CSC proportions were analyzed using Poisson distribution statistics and the L-Calc Version 1.1 software program (Stem Cell Technologies, Inc., Vancouver, Canada) as previously described (15).

In vivo limiting dilution assay

For the *in vivo* limiting dilution assay, miR-96 mimic or miR-96 sponge and their control hepatoma cells were mixed with Matrigel (BD) at a ratio of 1:1 and injected subcutaneously at indicated cell doses per NOD-SICD mouse (n=8). After 8 months, tumors formation was evaluated.

Real-time PCR

For detection of mature miR-96, total RNA was subjected to reverse transcription using a TaqMan MicroRNA Reverse Transcription Kit (Applied Biosystems). qRT-PCR analysis of miR-96 expression was carried out using TaqMan MicroRNA assay kits (Applied Biosystems). Results were normalized to U6 snRNA using the comparative threshold cycle (Ct) method.

The total RNA was extracted by using Trizol reagent (Invitrogen, 15596-018). Total cDNAs were synthesized by ThermoScript™ RT-PCR system (Invitrogen, 11146-057). The total mRNA amount present in the cells was measured by RT-PCR using the ABI PRISM 7300 sequence detector (Applied Biosystems). PCR conditions included 1 cycle at 94 °C for 5 minutes, followed by up to 40 cycles of 94 °C for 15 seconds (denaturation), 60 °C for 30 seconds (annealing) and 72 °C for 30 seconds (extension). The sequences of primers used was listed in Supplementary Table 1.

Western blotting assay

Thirty micrograms of proteins were subjected to sodium dodecyl sulfate polyacrylamide gel electrophoresis and then transferred to nitrocellulose membrane. The membrane was blocked with 5% non-fat milk and incubated with the primary antibody overnight. The protein band, specifically bound to the primary antibody, was detected using an IRDye 800CW-conjugated secondary antibody and LI-COR imaging system (LI-COR Biosciences, Lincoln, NE, USA). The primary antibodies used were listed in supplementary Table 2.

Luciferase reporter assay

Wild type and mutated SOX6 3'UTR was cloned to psiCHECK-2 Vector (Promega, Madison, WI, USA) to construct the psiCHECK-SOX6 3'UTR-wt and psiCHECK-SOX6 3'UTR-mut vectors with Lipofectamine 2000 Reagent (Invitrogen, Carlsbad, CA, USA). miR-96 sponge and its control hepatoma cells were transfected with SOX6 WT or SOX6 mutant 3'UTR plasmids for 48h. The luciferase activity was measured using a Synergy 2 Multidetector Microplate Reader (BioTek Instruments, Inc.). The data were normalized for transfection efficiency by dividing firefly luciferase activity by Renilla luciferase activity.

Apoptosis Assay

miR-96 mimic or miR-96 sponge and their control hepatoma cells were treated with sorafenib (10 μM) for 48 hours, followed by staining with Annexin V and 7-AAD for 15 minutes at 48C in the dark. Apoptotic cells were determined by an Annexin VFITC Apoptosis Detection Kit I (BD Pharmingen, San Diego, CA) and detected by flow cytometry according to the manufacturer's instructions.

Patient-derived xenograft

For the patient-derived xenograft (PDX) model, primary tumor samples were obtained for xenograft establishment as described previously. The mice with xenografts were given sorafenib (60 mg/kg) or vehicle daily orally for 24 days (n=5 for each group). Tumor volumes were measured at the end time

points. All procedures and protocols were approved by the Institutional Review Board of Eastern Hepatobiliary Surgery Hospital.

Statistical analysis

GraphPad Prism (GraphPad Software, Inc. La Jolla, USA) was used for all statistical analyses. Statistical analysis was carried out using t test or Bonferroni Multiple Comparisons Test: * $p < 0.05$. A p value of less than 0.05 was considered significant.

Results

The expression of miR-96 is upregulated in liver T-ICs.

It is well known that CD133 and EpCAM are liver T-ICs markers (16, 17). We isolated CD133 and EpCAM positive liver T-ICs from primary HCC patients and HCC cell lines. As shown in Fig. 1A&B, miR-96 expression was upregulated in CD133⁺ and EpCAM⁺ liver T-ICs that were sorted from primary HCC patients. Compared with the attached cells, miR-96 expression was increased in HCC spheres derived from human primary HCC cells (Fig. 1C). Consistently, miR-96 expression was also upregulated in CD133⁺ and EpCAM⁺ liver T-ICs that were sorted from HCC cell lines (Fig. 1D&E). Moreover, miR-96 expression was increased in the self-renewing spheroids compared with the attached cells (Fig. 1F). In serial passages of HCCLM3 or CSQT-2 spheroids, miR-96 expression was gradually increased (Fig. 1G). Taken together, these results demonstrated that miR-96 was preferentially upregulated in liver T-ICs.

miR-96 depletion suppresses liver T-ICs expansion.

To explore the biological function of miR-96 in liver T-ICs, HCCLM3 or CSQT-2 cells were infected with miR-96 sponge virus and the interference effect was confirmed by real-time PCR assay (Fig. 2A). Flow-cytometry analysis showed that EpCAM⁺ HCC cells was reduced in miR-96 knockdown hepatoma cells (Fig. 2B). Moreover, the expression of pluripotent transcription factors in miR-96 knockdown hepatoma cells was downregulated (Fig. 2C&D). Additionally, miR-96 interference hepatoma cells formed smaller and fewer spheroids than control cells (Fig. 2E). Furthermore, in vitro and in vivo limiting dilution assay revealed that suppression of miR-96 significantly reduced T-ICs frequency and tumorigenesis ability in hepatoma cells (Fig. 2F&G).

miR-96 promotes liver T-ICs expansion.

To further explore the role of miR-96 in liver T-ICs, HCCLM3 or CSQT-2 cells were infected with miR-96 mimic virus and the overexpress effect was confirmed by real-time PCR assay (Fig. 3A). Flow-cytometry analysis showed that EpCAM⁺ HCC cells was increased in miR-96 overexpressing hepatoma cells (Fig. 3B). Moreover, the expression of pluripotent transcription factors in miR-96 overexpressing hepatoma cells was upregulated (Fig. 3C&D). Additionally, miR-96 overexpressing hepatoma cells formed much more spheroids than control cells (Fig. 3E). Furthermore, in vitro and in vivo limiting dilution assay

revealed that overexpression of miR-96 significantly increased T-ICs frequency and tumorigenesis ability in hepatoma cells (Fig. 3F&G).

SOX6 is required for miR-96 mediated T-ICs expansion.

It was reported that miR-96 targeted the 3'-UTR of SOX6, FOXO1 and FOXO3a in hepatoma cells (18, 19). So, we doubted whether SOX6, FOXO1 and FOXO3a was involved in miR-96 mediated liver T-ICs expansion. Our data found that FOXO1 and FOXO3a expression was unchanged in miR-96 knockdown liver T-ICs. However, SOX6 mRNA expression was increased in miR-96 knockdown liver T-ICs (Fig. 4A). Consistently, the SOX6 protein level was also upregulated in miR-96 knockdown liver T-ICs (Fig. 4B). To further explore whether miR-96 directly regulates SOX6 expression via interaction with its 3'-UTR, the wild-type or mutant SOX6 3'-UTR reporter plasmids were transfected into miR-96 interference hepatoma cells. The mutation of miR-96 binding site in the SOX6 3'-UTR diminished the distinct activation of SOX6 3'-UTR between miR-96 knockdown cells and control cells (Fig. 4C). Consistently, there was a significant negative correlation between miR-96 and SOX6 mRNA expression in HCC samples (Fig. 4D). To further confirm the role of SOX6 in miR-96-mediated liver T-ICs expansion, the SOX6 siRNA was used (Fig. 4E). SOX6 siRNA diminished the discrepancy of expression of T-ICs markers, self-renewal ability, and tumorigenesis capacity between miR-96 knockdown hepatoma cells and control cells (Fig. 4F-H).

miR-96 overexpression HCC cells are resistant to sorafenib treatment.

Increasing evidence shows that liver T-ICs were closely associated with HCC chemoresistance. Thus, we next explored the correlation between miR-96 expression and sorafenib response in HCC patients. miR-96 expression was significantly upregulated in sorafenib-resistant HCC xenografts (Fig. 5A). Consistently, we also found that miR-96 expression was increasing in sorafenib-resistant hepatoma cells (Fig. 5B). miR-96 overexpression led to the resistance of hepatoma cells upon sorafenib-induced cell apoptosis (Fig. 5C). Moreover, miR-96 knockdown sensitized hepatoma cells to sorafenib-induced cell apoptosis (Fig. 5D). In addition, western blot analysis also showed that the protein expression of cleaved-PARP in miR-96 overexpressing hepatoma cells was decreased when they were exposed to the same doses of sorafenib (Fig. 5E). Furthermore, we found that the PDXs derived from HCC tumors with high miR-96 levels were resistant to sorafenib treatment. In contrast, sorafenib eliminated the growth of PDXs derived from the HCC tumors with low miR-96 levels compared with the vehicle controls (Fig. 5F&G), further demonstrating that the miR-96 expression in HCC patients can serve as a reliable predictor for sorafenib response.

Discussion

Most cancer therapies fail to eradicate tumors due to the existence of T-ICs. However, the understanding of regulatory mechanisms for T-ICs is limited. In the present study, we demonstrated the critical role of miR-96 in liver T-ICs and the underlying mechanism. To our knowledge, this is the first report for miR-96 in the regulation of liver T-ICs.

Accumulating evidence shows that miRNAs are involved in the regulation of human cancers and can be used as the diagnosis and therapeutic targets (20, 21). For instance, miR-96 is upregulated in breast cancer and promotes breast cancer metastasis by suppressing MTSS1 (22). It was also reported that miR-96 works as a tumor repressor by inhibiting NPTX2 in renal cell carcinoma (23). However, the potential function of miR-96 in liver T-ICs has not been reported. In the present study, we found that miR-96 expression is significantly upregulated in CD133⁺ or EpCAM⁺ primary liver T-ICs. Moreover, miR-96 can promote the self-renewal capacity and tumorigenicity of liver T-ICs.

The existence of T-ICs has been confirmed by numerous studies, and these cells have the ability to self-renew and the potential for generating heterogeneous malignant progenies (24, 25). It was well-accepted that liver T-ICs were closely associated with the chemoresistance and HCC recurrence. In this study, liver T-ICs were enriched by establishing chemo-resistant HCC xenograft tumors, and expression of miR-96 in these chemo-resistant xenografts was dramatically increased. Spheroid culture of cancer cells is a routine approach to enrich T-ICs. We also found that miR-96 expression was upregulated in human primary hepatoma spheroids. CD133⁺ or EpCAM⁺ are well-known liver T-ICs markers. Our data showed that miR-96 levels increased in CD133⁺ or EpCAM⁺ primary liver T-ICs. Moreover, knockdown miR-96 inhibited the self-renewal ability and tumorigenesis capacity of liver T-ICs. Conversely, miR-96 overexpression promoted liver T-ICs self-renew and tumorigenesis. Sorafenib is the first FDA-approved targeted drug which was used for the treatment of advanced HCC patients (26, 27). However, only a small part of HCC patients is benefited from sorafenib treatment. Therefore, it is important to find the right population of patients for sorafenib treatment. In this study, our finding revealed that miR-96 knockdown HCC cells are more sensitive to sorafenib treatment. PDX studies further confirmed that low miR-96 level in HCC patients can serve as a reliable predictor for sorafenib response.

It was widely recognized that SOX6 gene is an important tumor suppressor. SOX6 suppressed number cancers initiation and progression (28–30). Previous studies have elucidated that SOX6 plays essential roles in HCC. For instance, SOX6 was downregulated in HCC tissues and predicted the poor prognosis of HCC patients (31). miR-155 promotes HCC cells tumorigenesis partly through the miR-155/SOX6/p21waf1/cip1 axis (32). In addition, SOX6 was reported to be involved in the regulation of cancer stemness (33). We hereby revealed that knockdown miR-96 upregulated SOX6 mRNA and protein expression in liver T-ICs. Moreover, we found that miR-96 directly regulates SOX6 expression via interaction with its 3'-UTR. SOX6 siRNA further confirm that miR-96 via SOX6 pathway promotes liver T-ICs expansion.

Conclusion

We demonstrated for the first time that miR-96 expression is upregulated in liver T-ICs, and miR-96 shRNA silencing suppresses the self-renewal and tumorigenesis of liver T-ICs. Moreover, miR-96 promoted liver T-ICs expansion by directly targeting SOX6. The findings of the present study not only shed new light on the mechanisms responsible for liver T-ICs expansion but also suggest that miR-96 may be a potential therapeutic target for liver T-ICs.

Abbreviations

T-ICs: tumor-initiating cells; CSCs: cancer stem cells; miRNAs: MicroRNAs; HCC: hepatocellular carcinoma; 3'-UTR: 3'-untranslational region; DMEM: Dulbecco's modified Eagle's medium; FBS: fetal bovine serum; APC: adenomatous polyposis coli; PDXs: patient-derived xenografts.

Declarations

Ethics approval and consent to participate:

All procedures performed in studies involving human participants and animals were in accordance with the ethical standards of the institutional and/or national research committee and with the 1964 Helsinki declaration and its later amendments or comparable ethical standards. All of the patients provided signed informed consent. The Ethics Committee of Eastern Hepatobiliary Surgery Hospital approved the retrieval method for cancer specimens.

Consent for publication:

Agree.

Availability of data and materials:

Data generated from the study are available from the corresponding author on reasonable request.

Competing interests:

All authors declare no competing interests.

Funding:

This work was supported by grants from the National Natural Science Foundation of China (81572791, 81101578), Kunshan science and technology development project (KS19045). The funding was used in the design of the study and collection, analysis, and interpretation of data and in writing the manuscript.

Authors' contributions:

Yonggang Huang, Jin Zhang and Wei Dong conducted all experiments and analyzed the data. Yonggang Huang and Huiping Peng wrote the manuscript and Maolin Gu and Hengjie Wang contributed to the revision. Maolin Gu and Hengjie Wang conceived the project and supervised all experiments. All authors read and approved the final manuscript.

Acknowledgements

We thank Junyu Liu for technical assistance.

References

1. Forner A, Reig M, Bruix J. Hepatocellular carcinoma. *Lancet* 2018;391:1301-1314.
2. Xiang DM, Sun W, Zhou T, Zhang C, Cheng Z, Li SC, Jiang W, et al. Oncofetal HLF transactivates c-Jun to promote hepatocellular carcinoma development and sorafenib resistance. *Gut* 2019;68:1858-1871.
3. Magee JA, Piskounova E, Morrison SJ. Cancer stem cells: impact, heterogeneity, and uncertainty. *Cancer Cell* 2012;21:283-296.
4. Li XF, Chen C, Xiang DM, Qu L, Sun W, Lu XY, Zhou TF, et al. Chronic inflammation-elicited liver progenitor cell conversion to liver cancer stem cell with clinical significance. *Hepatology* 2017;66:1934-1951.
5. Yang W, Yan HX, Chen L, Liu Q, He YQ, Yu LX, Zhang SH, et al. Wnt/beta-catenin signaling contributes to activation of normal and tumorigenic liver progenitor cells. *Cancer Res* 2008;68:4287-4295.
6. Yang ZF, Ho DW, Ng MN, Lau CK, Yu WC, Ngai P, Chu PW, et al. Significance of CD90+ cancer stem cells in human liver cancer. *Cancer Cell* 2008;13:153-166.
7. Tutar Y. miRNA and cancer; computational and experimental approaches. *Curr Pharm Biotechnol* 2014;15:429.
8. Hessam S, Sand M, Skrygan M, Gambichler T, Bechara FG. Expression of miRNA-155, miRNA-223, miRNA-31, miRNA-21, miRNA-125b, and miRNA-146a in the Inflammatory Pathway of Hidradenitis Suppurativa. *Inflammation* 2017;40:464-472.
9. Zhou SL, Hu ZQ, Zhou ZJ, Dai Z, Wang Z, Cao Y, Fan J, et al. miR-28-5p-IL-34-macrophage feedback loop modulates hepatocellular carcinoma metastasis. *Hepatology* 2016;63:1560-1575.
10. Sun CC, Li SJ, Yuan ZP, Li DJ. MicroRNA-346 facilitates cell growth and metastasis, and suppresses cell apoptosis in human non-small cell lung cancer by regulation of XPC/ERK/Snail/E-cadherin pathway. *Aging (Albany NY)* 2016;8:2509-2524.
11. Bartolome-Izquierdo N, de Yébenes VG, Alvarez-Prado AF, Mur SM, Lopez Del Olmo JA, Roa S, Vazquez J, et al. miR-28 regulates the germinal center reaction and blocks tumor growth in preclinical models of non-Hodgkin lymphoma. *Blood* 2017;129:2408-2419.

12. Zhao X, Li Y, Zhou Y. MicroRNA-96-3p promotes metastasis of papillary thyroid cancer through targeting SDHB. *Cancer Cell Int* 2019;19:287.
13. Ding H, Chu M, Yue J, Huang H, Wang J, Zhu L. MiR-96 induced non-small-cell lung cancer progression through competing endogenous RNA network and affecting EGFR signaling pathway. *Iran J Basic Med Sci* 2019;22:908-914.
14. Han T, Xiang DM, Sun W, Liu N, Sun HL, Wen W, Shen WF, et al. PTPN11/Shp2 overexpression enhances liver cancer progression and predicts poor prognosis of patients. *J Hepatol* 2015;63:651-660.
15. Xiang D, Cheng Z, Liu H, Wang X, Han T, Sun W, Li X, et al. Shp2 promotes liver cancer stem cell expansion by augmenting beta-catenin signaling and predicts chemotherapeutic response of patients. *Hepatology* 2017;65:1566-1580.
16. Ma S, Lee TK, Zheng BJ, Chan KW, Guan XY. CD133+ HCC cancer stem cells confer chemoresistance by preferential expression of the Akt/PKB survival pathway. *Oncogene* 2008;27:1749-1758.
17. Yamashita T, Ji J, Budhu A, Forgues M, Yang W, Wang HY, Jia H, et al. EpCAM-positive hepatocellular carcinoma cells are tumor-initiating cells with stem/progenitor cell features. *Gastroenterology* 2009;136:1012-1024.
18. Li Z, Wang Y. miR-96 targets SOX6 and promotes proliferation, migration, and invasion of hepatocellular carcinoma. *Biochem Cell Biol* 2018;96:365-371.
19. Xu D, He X, Chang Y, Xu C, Jiang X, Sun S, Lin J. Inhibition of miR-96 expression reduces cell proliferation and clonogenicity of HepG2 hepatoma cells. *Oncol Rep* 2013;29:653-661.
20. Cheng G. Circulating miRNAs: roles in cancer diagnosis, prognosis and therapy. *Adv Drug Deliv Rev* 2015;81:75-93.
21. Negoita SI, Sandesc D, Rogobete AF, Dutu M, Bedreag OH, Papurica M, Ercisli MF, et al. miRNAs Expressions and Interaction with Biological Systems in Patients with Alzheimer`s Disease. Using miRNAs as a Diagnosis and Prognosis Biomarker. *Clin Lab* 2017;63:1315-1321.
22. Xie W, Sun F, Chen L, Cao X. miR-96 promotes breast cancer metastasis by suppressing MTSS1. *Oncol Lett* 2018;15:3464-3471.
23. Xiang W, Han L, Mo G, Lin L, Yu X, Chen S, Gao T, et al. MicroRNA-96 is a potential tumor repressor by inhibiting NPTX2 in renal cell carcinoma. *J Cell Biochem* 2020;121:1504-1513.
24. Park JR, Kim RJ, Lee YK, Kim SR, Roh KJ, Oh SH, Kong G, et al. Dysadherin can enhance tumorigenesis by conferring properties of stem-like cells to hepatocellular carcinoma cells. *J Hepatol* 2011;54:122-131.
25. Xiong Y, Fang JH, Yun JP, Yang J, Zhang Y, Jia WH, Zhuang SM. Effects of microRNA-29 on apoptosis, tumorigenicity, and prognosis of hepatocellular carcinoma. *Hepatology* 2010;51:836-845.
26. Horwitz E, Stein I, Andreozzi M, Nemeth J, Shoham A, Pappo O, Schweitzer N, et al. Human and mouse VEGFA-amplified hepatocellular carcinomas are highly sensitive to sorafenib treatment. *Cancer Discov* 2014;4:730-743.

27. Arao T, Ueshima K, Matsumoto K, Nagai T, Kimura H, Hagiwara S, Sakurai T, et al. FGF3/FGF4 amplification and multiple lung metastases in responders to sorafenib in hepatocellular carcinoma. *Hepatology* 2013;57:1407-1415.
28. Jiang W, Yuan Q, Jiang Y, Huang L, Chen C, Hu G, Wan R, et al. Identification of Sox6 as a regulator of pancreatic cancer development. *J Cell Mol Med* 2018;22:1864-1872.
29. Li Y, Xiao M, Guo F. The role of Sox6 and Netrin-1 in ovarian cancer cell growth, invasiveness, and angiogenesis. *Tumour Biol* 2017;39:1010428317705508.
30. Yu Y, Wang Z, Sun D, Zhou X, Wei X, Hou W, Ding Y, et al. miR-671 promotes prostate cancer cell proliferation by targeting tumor suppressor SOX6. *Eur J Pharmacol* 2018;823:65-71.
31. Guo X, Yang M, Gu H, Zhao J, Zou L. Decreased expression of SOX6 confers a poor prognosis in hepatocellular carcinoma. *Cancer Epidemiol* 2013;37:732-736.
32. Xie Q, Chen X, Lu F, Zhang T, Hao M, Wang Y, Zhao J, et al. Aberrant expression of microRNA 155 may accelerate cell proliferation by targeting sex-determining region Y box 6 in hepatocellular carcinoma. *Cancer* 2012;118:2431-2442.
33. Ohta S, Misawa A, Lefebvre V, Okano H, Kawakami Y, Toda M. Sox6 up-regulation by macrophage migration inhibitory factor promotes survival and maintenance of mouse neural stem/progenitor cells. *PLoS One* 2013;8:e74315.

Figures

Figure 1

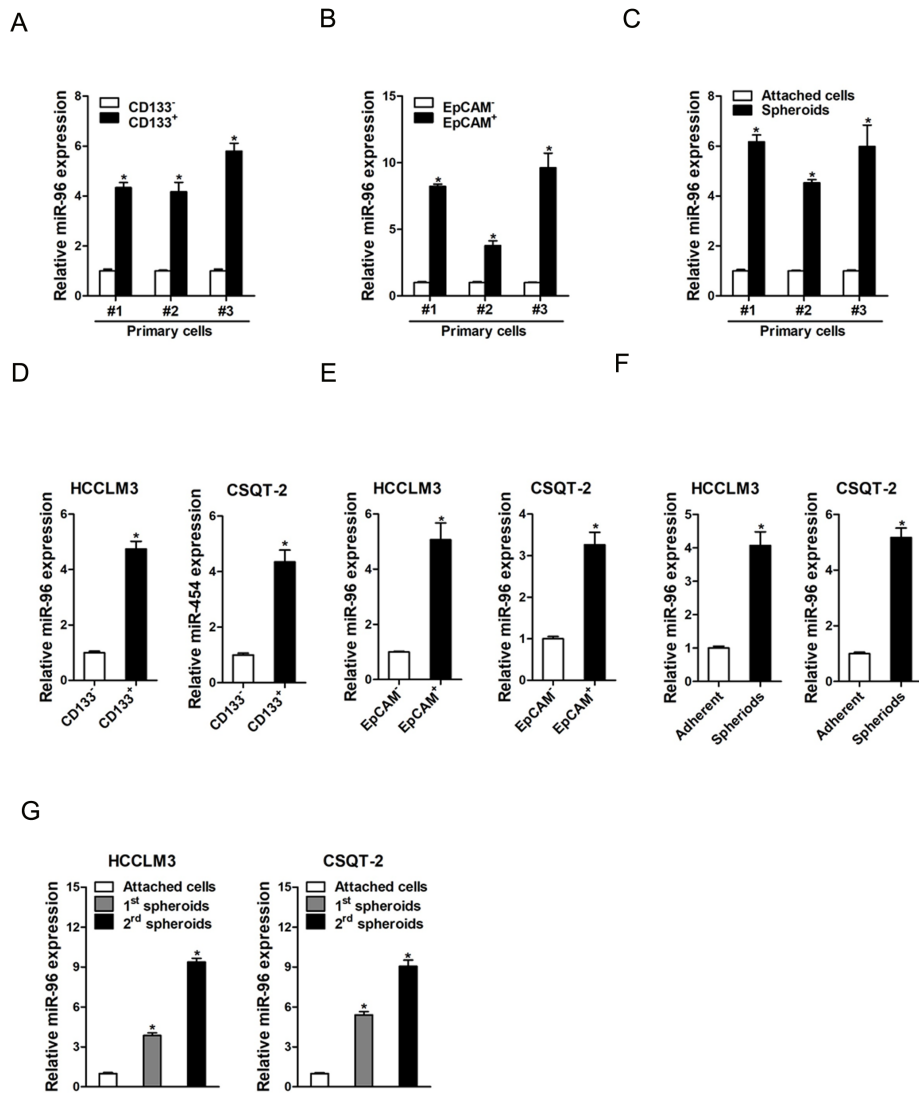


Figure 1

miR-96 is upregulated in liver T-ICs. A. The expression of miR-96 in MACS sorted CD133+ primary HCC cells was checked by real-time PCR assay. (n=3) B. The expression of miR-96 in MACS sorted EpCAM+ primary HCC cells was checked by real-time PCR assay. (n=3) C. The expression of miR-96 in primary HCC adherent and spheroids cells was checked by real-time PCR assay. (n=3) D. Real-time PCR was performed to check the expression of miR-96 in MACS sorted CD133+ HCC cells. (n=3) E. Real-time PCR

was performed to check the expression of miR-96 in MACS sorted EpCAM+ HCC cells. (n=3) F. Real-time PCR was performed to check the expression of miR-96 in HCC adherent and spheroids cells. (n=3) G. miR-96 expression in serial passages of HCCLM3 and CSQT-2 spheroids was analyzed by real-time PCR. (n=3) (Data are represented as mean±s.d.; *P<0.05; two-tailed Student's t-test.)

Figure 2

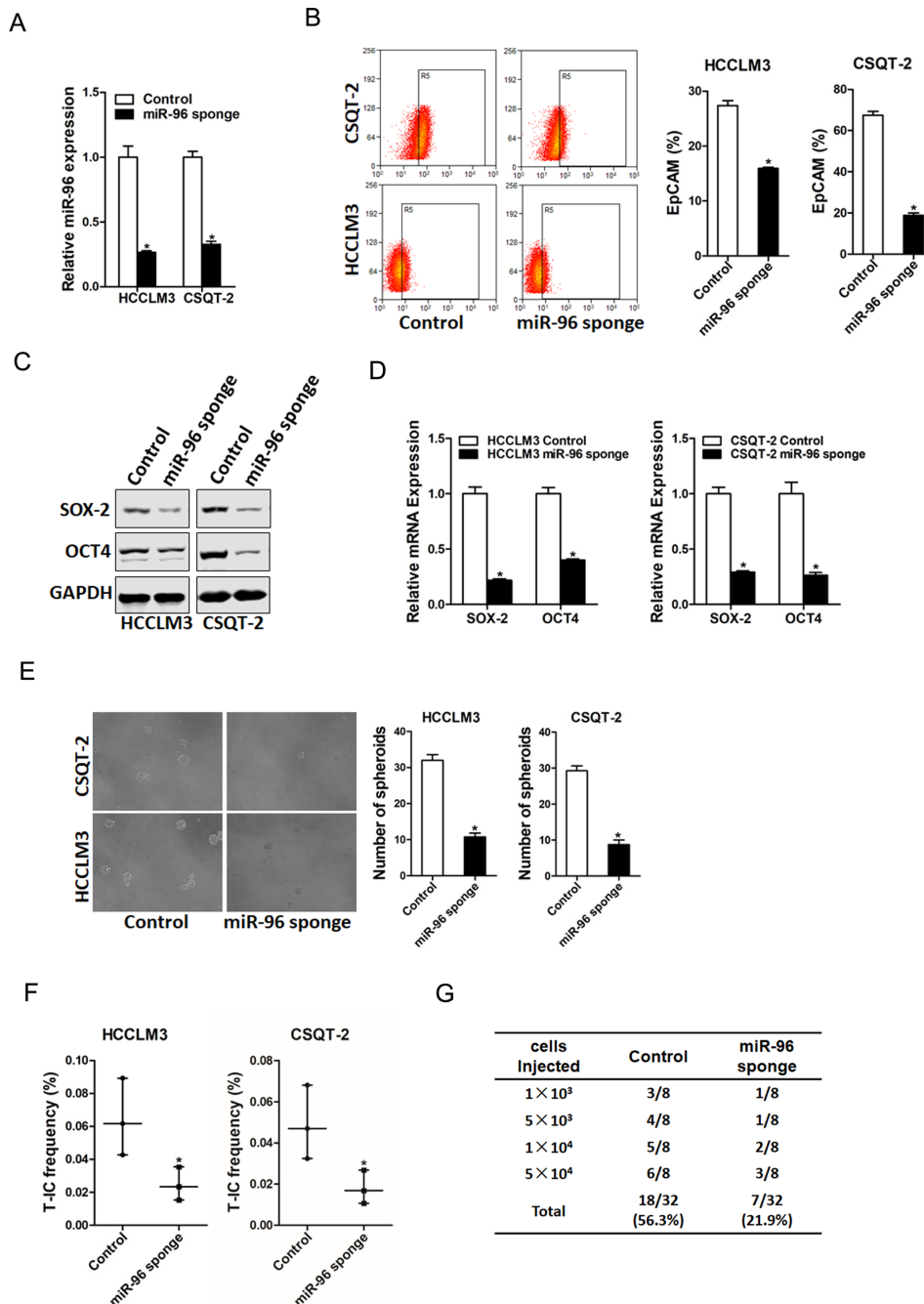


Figure 2

miR-96 knockdown inhibits liver T-ICs expansion. A. HCCLM3 and CSQT-2 cells were infected with miR-96 sponge virus and the stable infectants were determined by real-time PCR. (n=3) B. The expression of liver T-ICs surface marker EpCAM miR-96 sponge and control hepatoma cells was checked by flow-cytometry analyses. (n=3) C. The protein expression of SOX-2 and OCT4 was checked in miR-96 sponge and control hepatoma cells. (n=3) D. The mRNA expression of SOX-2 and OCT4 was checked in miR-96 sponge and control hepatoma cells. (n=3) E. Spheres formation assay of miR-96 sponge and control hepatoma cells. (n=3) F. The frequency of liver T-ICs in miR-96 sponge and control hepatoma cells was compared by in vitro limiting dilution assay. (n=16) G. The frequency of liver T-ICs in miR-96 sponge and control hepatoma cells was compared by in vivo limiting dilution assay. (n=8) (Data are represented as mean±s.d.; *P<0.05; two-tailed Student's t-test.)

Figure 3

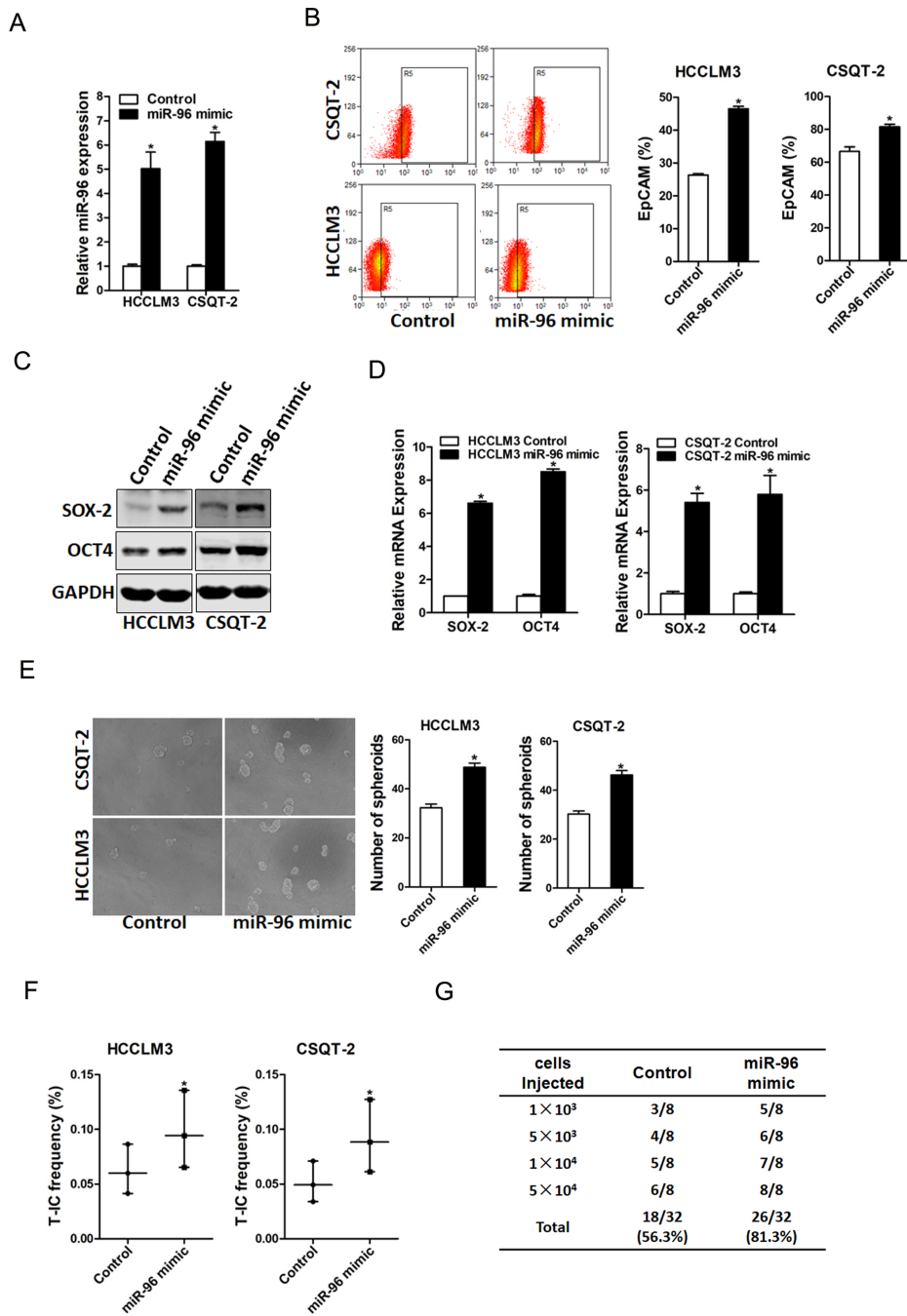


Figure 3

miR-96 overexpression promotes the expansion of liver T-ICs. A. HCCLM3 and CSQT-2 cells were infected with miR-96 mimic virus and the stable infectants were determined by real-time PCR. (n=3) B. The expression of liver T-ICs surface marker EpCAM miR-96 mimic and control hepatoma cells was checked by flow-cytometry analyses. (n=3) C. The protein expression of SOX-2 and OCT4 was checked in miR-96 mimic and control hepatoma cells. (n=3) D. The mRNA expression of SOX-2 and OCT4 was checked in

miR-96 mimic and control hepatoma cells. (n=3) E. Spheres formation assay of miR-96 mimic and control hepatoma cells. (n=3) F. The frequency of liver T-ICs in miR-96 mimic and control hepatoma cells was compared by in vitro limiting dilution assay. (n=16) G. The frequency of liver T-ICs in miR-96 mimic and control hepatoma cells was compared by in vivo limiting dilution assay. (n=8) (Data are represented as mean±s.d.; *P<0.05; two-tailed Student's t-test.)

Figure 4

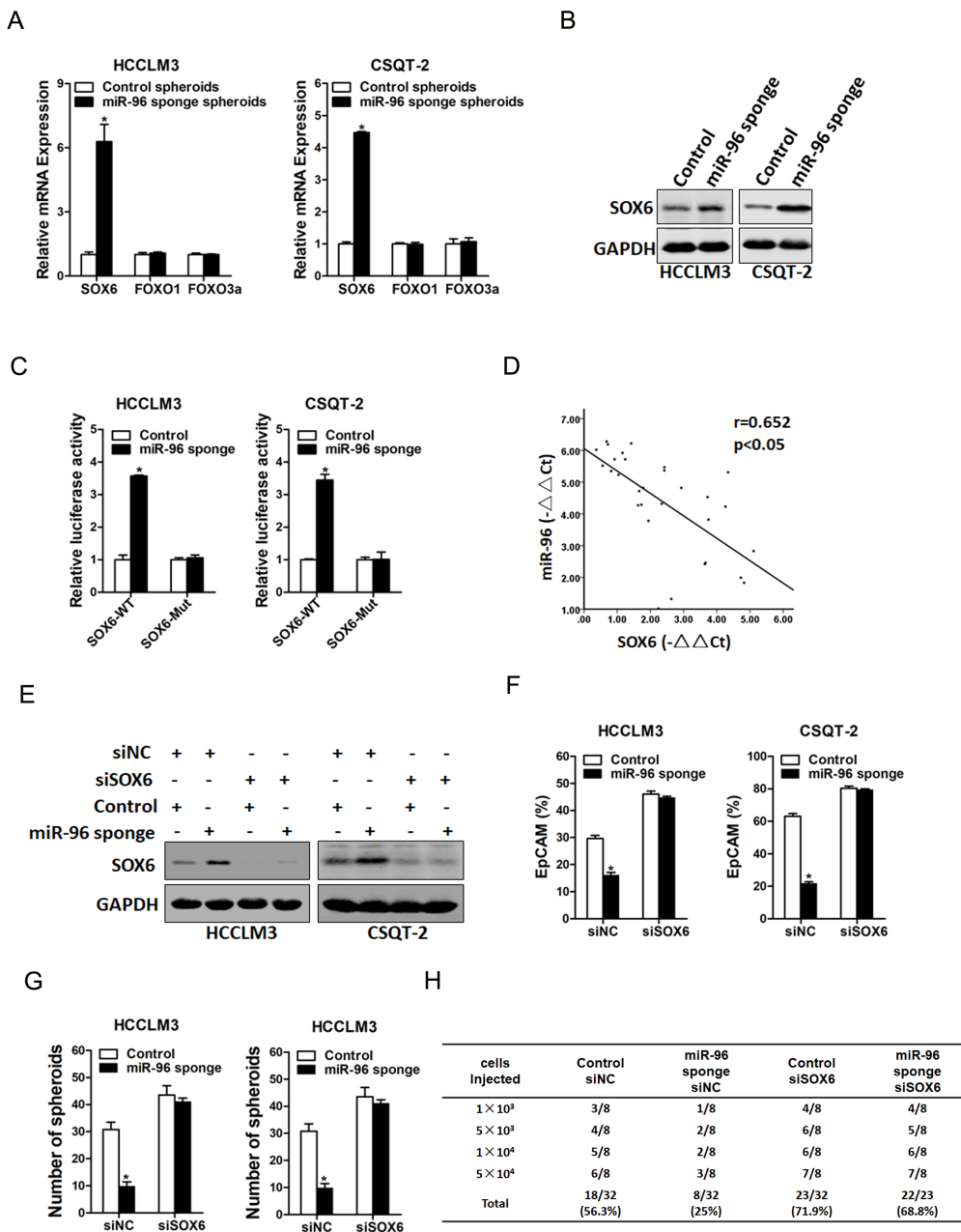


Figure 4

SOX6 is a direct target of miR-96 in liver TICs. A. The mRNA of SOX6, FOXO1 and FOXO3a in miR-96 sponge spheroids and control hepatoma spheroids was determined by real-time PCR assay. (n=3) B. The protein expression of SOX6 in miR-96 sponge spheroids and control hepatoma spheroids was checked by western blot assay. C. Luciferase reporter assays performed in miR-96 sponge and control cells transfected with wild-type or mutant SOX6 3'-UTR constructs. (n=3) D. Spearman correlation analysis of the relationship between SOX6 mRNA and miR-96 expression in 30 HCC specimens. E. miR-96 sponge and control hepatoma cells were transfected with SOX6 siRNA or control siRNA and subjected to western blot assay. (n=3) F. miR-96 sponge and control hepatoma cells were transfected with SOX6 siRNA or control siRNA and the EpCAM+ hepatoma cells were checked by flow-cytometric assay. (n=3) G. miR-96 sponge and control hepatoma cells were transfected with SOX6 siRNA or control siRNA and subjected to spheroid formation. (n=3) H. miR-96 sponge and control hepatoma cells were transfected with SOX6 siRNA or control siRNA and were then injected subcutaneously into NOD-SCID mice. Tumors incidence was observed over 2 months; n=8 for each group. (Data are represented as mean±s.d.; *P<0.05; two-tailed Student's t-test.)

Figure 5

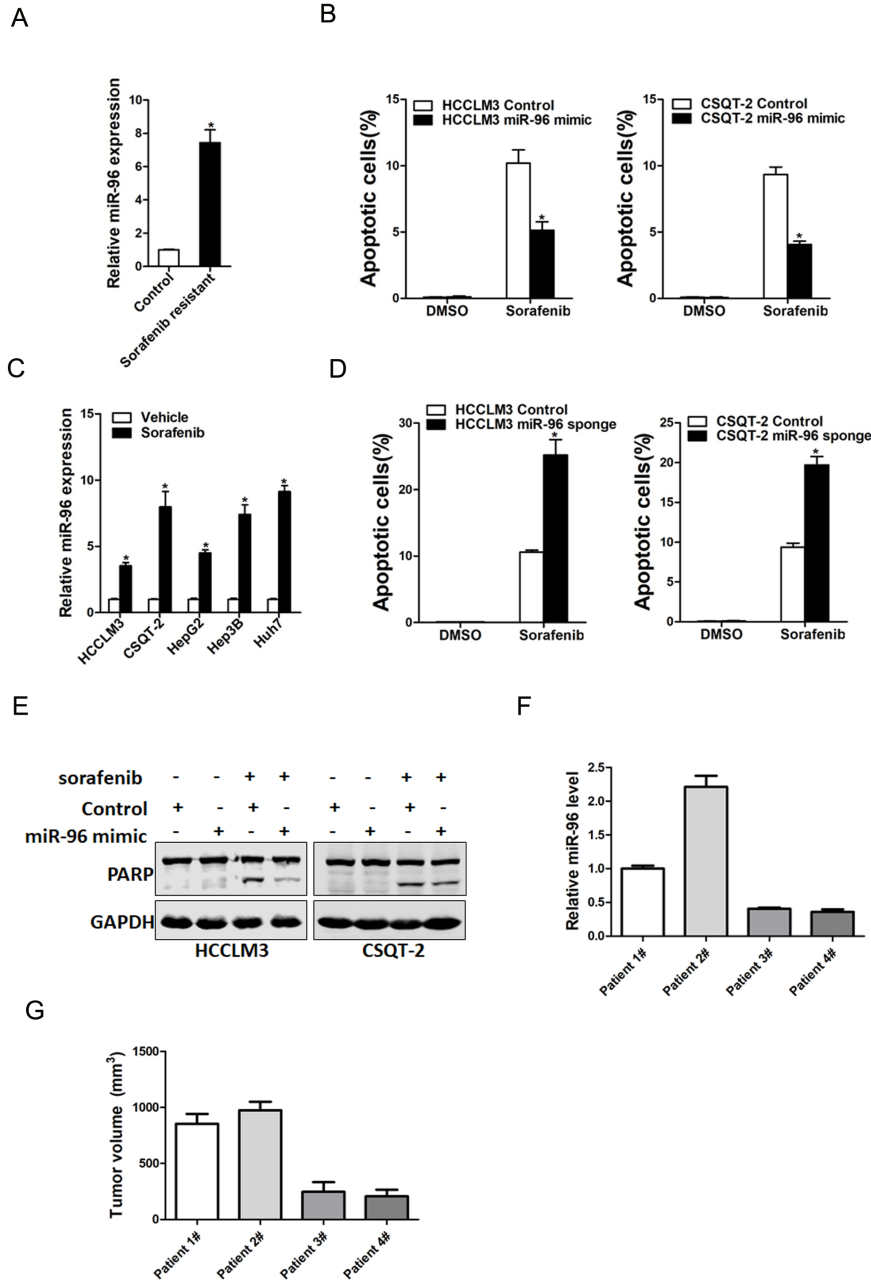


Figure 5

miR-96 is associated with the sensitivity of sorafenib. A. The expression of miR-96 in sorafenib resistant PDXs were checked by real-time PCR assay. (n=6) B. The expression of miR-96 in sorafenib resistant HCC cell lines were checked by real-time PCR assay. (n=3) C. miR-96 mimic and control hepatoma cells were treated with sorafenib (10 μ M) for 48 hours and their apoptosis was checked by flow cytometry. (n=3) D. miR-96 sponge and control hepatoma cells were treated with sorafenib (10 μ M) for 48 hours and their

apoptosis was checked by flow cytometry. (n=3) E. miR-96 mimic and control hepatoma cells were treated with 10 μ M sorafenib as indicated for 48 hours. The protein of cleaved-PARP was determined by western blot. F. The expression of miR-96 in PDXs primary tumors was determined by RT-PCR assay. (n=4) G. PDXs with low or high miR-96 expression in their primary tumors were treated with sorafenib (60 mg/kg body weight) or vehicle for 30 days (n=6 for each group). The terminal tumor size and weight was showed. (Data are represented as mean \pm s.d.; *P \leq 0.05; two-tailed Student's t-test.)

Supplementary Files

This is a list of supplementary files associated with this preprint. Click to download.

- [supplementary.docx](#)